Thrust Area 4: Solar (Thermal)

Solar Thermal Power for Bulk Power and Distributed Generation

PI: David W. Hahn **Co-PIs:** James Klausner, Renwei Mei, Helena Weaver
Students: Richard Stehle (PhD); Michael Bobek (PhD); Kyle Allen (PhD);
Justin Dodson (PhD), Like Li (PhD)

Description: While there are many different approaches to hydrogen generation, the most attractive means is to split water molecules using solar energy. The current approach is to develop highly reactive metal oxide materials to produce intermediary reactions that result in the splitting of water to produce hydrogen at moderate temperatures (<1000 K). It is envisioned that the metal oxide reactors will ultimately be mounted within a solar concentrating reactor, and irradiated via heliostats. This Task is structured toward the overall goals of solar-driven, thermochemical hydrogen production, with associated efforts toward the enabling surface science, catalysis, particle science, material synthesis, nano-structures, multiscale-multiphase physics modeling, and process simulation that will enable the realization of solar hydrogen-based fuels to power the transportation economy. Successful efforts as targeted in this project are a critical step toward increased renewable-resource based fuels and energy, reduction of greenhouse gas emissions, and establishment of a new power industry in Florida.

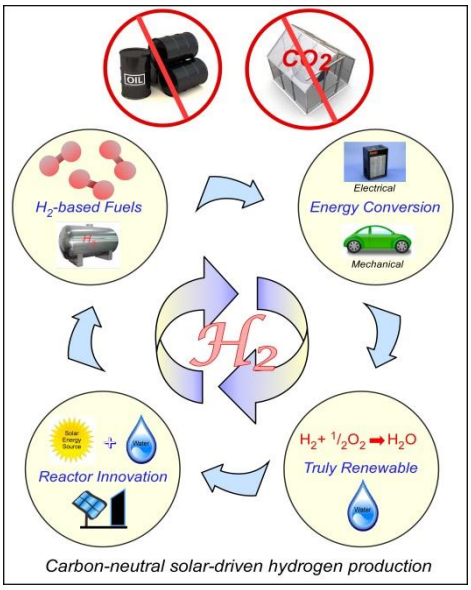

Carbon-neutral solar-driven hydrogen production

.

Budget: $446,000
Universities: UF

Progress Summary

As previously reported the effort has focused on the experimental activity of two thermal reactors for fundamental studies of the reactor processes and surface chemistry for hydrogen production. The first reactor has a monolithic configuration in order to obtain fundamental reaction kinetics for the oxidation and reduction of the metal ferrite. The second reactor design is configured around the concept of a fluidized bed to achieve high efficiency with actual reactors. As of the current date, initial work into the basic mechanisms that represent the oxidation of iron into the iron oxide magnetite (Fe_3O_4) has been completed and investigation into regenerative cycles has commenced.

From the experimental data for iron oxidation in the temperature range of 600K – 850K, the activation energy associated with this hydrogen producing step correlates to the dissociation energy of water molecules on a chemisorption surface. This activation energy is representative of the kinetically limited regime for the oxidation reaction which follows the initial transient induction period. This result is used for initial consideration into the length of reaction for the oxidation step and to help characterize the corresponding regenerating reduction step.

At present, the regenerative cycle approach has been optimized based on experimental data from iron oxidation along with experimental approaches into the cycling process. The length of the oxidation step is intended to last the extent of the transient reaction period but concluded before steady state

hydrogen production is reached. Reduction takes place to regenerate the vacancies lost during oxidation. The length of this step aims to correlate to the amount of oxygen adsorbed during hydrogen production.

Additional efforts have focused on understanding of surface reaction processes and the relationships between surface properties and functionality, specifically the comparisons of the properties at the end of the oxidation and reduction steps; and clarifying mechanistic details of the surface reactions.

At present, the fluidized bed rector is complete and has undergone testing and has now been used for extensive experimental investigations under actual hydrogen production conditions. The reactor was constructed about a high-temperature tube furnace to provide uniform process heat. A reduced iron-oxide power was used for assessment of the reactor performance, including assessment of magnetically-assisted fluidization. On-line mass spectrometry was used to quantify hydrogen production over a range of conditions.

Furthermore, preliminary thermo-gravimetric analysis data associated with particle sintering indicated that iron oxide supported on nanoparticle zirconium oxide (n-ZrO_2) and nanoparticle yttria-stabilized zirconium oxide (n-ZrO_2(Y_2O_3) with 8% Y_2O_3) are promising combinations in the two-step water splitting reaction. After being heated to 1500°C both catalysts remained as powders rather than sintering into solid blocks. These catalysts were therefore characterized further to determine the effect of high temperatures on the catalysts.

Finally, computational activities are focused on the fluidized bed, in which critical transport phenomena are being addressed with regard to scaling to larger processes or to solar-driven processes.

Funds leveraged/new partnerships created:

Received 2011 ARPA-E award for $2.975M. James Klausner is PI, D.W. Hahn, R. Mei, and J. Petrasch are co-PIs. Title: Thermal Fuel: Solar Thermochemical Fuel Production via a Novel Low Pressure, Magnetically Stabilized, Non-volatile Iron Oxide Looping Process

2011 Annual Report

Our project efforts to date have focused on direct hydrogen splitting from water in support of our overall mission to conceive, design, and develop advanced reactor technologies that utilize concentrated solar energy and highly reactive materials to produce low cost hydrogen. These activities directly align with the National Academy of Engineering Grand Challenge and published DOE strategic goals.

High temperature thermochemical production of hydrogen that uses concentrated solar radiation for process heat has been suggested as a candidate technology for renewable hydrogen. This process entails a two-step approach where endothermic dissociation of a metal oxide is driven in a solar furnace. The liberated metal (or reduced metal oxide) is mixed with water vapor, and the resulting exothermic reaction liberates hydrogen molecules and re-oxidizes the metal. The metal oxide decomposition requires very high temperatures, on the order of 1500 C. The advantage of the two-step process is that the high-temperature separation of H_2 and O_2 is avoided and no explosive H_2 and O_2 mixtures are formed, since the H_2 and O_2 are formed in different steps. Current technological hurdles to achieving successful hydrogen production are the high operating temperatures needed to

achieve reasonable reaction kinetics, cyclic stability of the reactive material, non-uniform transient heating, and recuperation of thermal energy lost through high temperature operation. In order to overcome these technological hurdles, our FESC team has specifically initiated a plan to revolutionize thermochemical reactor design through the development of magnetically fluidized bed reactors. There are many technological advantages to operating such a reactor including, very high reaction surface area to yield rapid kinetics at more moderate operating temperatures (<1000 K), more spatially uniform temperature distribution during transient heating, and substantial control over the fluidization characteristics of the bed using magnetic fields. For the reactor temperature operating regime, the most likely phase transition during the iron oxidation process is a conversion of iron powder to magnetite. Both have excellent magnetic properties and are easily fluidized using electromagnets. Activities for the past year have focused extensively on experimental characterization of key process kinetics and on reactor design, with supporting modeling efforts and fundamental catalysis studies.

Fundamental Kinetics Study

During this reporting period, the thermal reactor that was built and reported on in the previous report was used extensively to finalize our investigation into the reaction kinetics for the oxidation of iron to magnetite. The results from the study have been published in the International Journal of Hydrogen Energy and are illustrated in the figures below. Figure 1 is a schematic of our reactor and can help further visualize the oxidation process. A change that needs to be noted in relation to the reactor conditions that were reported that year corresponds to temperature measurements.

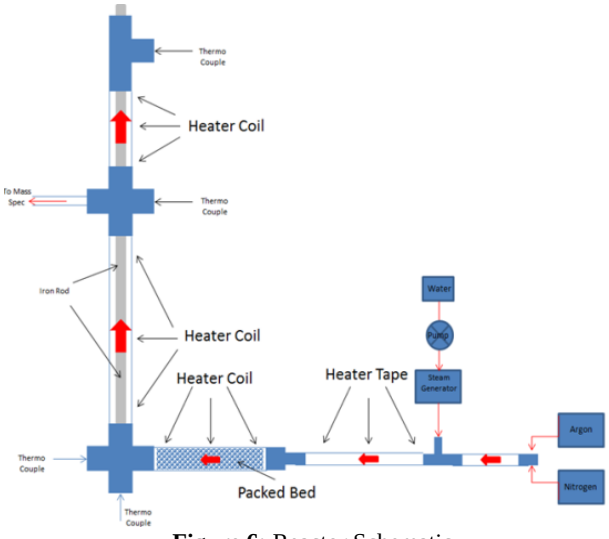

Figure 6: Reactor Schematic

Previously it was mentioned that our reactor operated at four distinct temperatures of 600, 650, 700 and 750k, but these temperatures were in correctly measured and have been reiterated for temperatures of 690, 740, 790 and 840k. The system continued to operate under constant flows of inert nitrogen (100cc/min) and argon (200cc/min) along with an input of vaporized water (~12.5cc/min) for approximately 3 hours. The results of the oxidation experiments can be seen in figure 2 as a relation of hydrogen production rate vs. Temperature and in figure 3 as an effective arrhenius form. What's important to note from figure 2 is not only the increase in production rate as temperature increases but also the effect time has on the production. There are 3 distinct limiting

regimes that correlate to production rate and more importantly to oxide production. The first regime occurs in very short intervals (<5 min) and is not identified in figure 2 but can be expressed in the numerical data. This initial oxidation period is very transient and spontaneous in relation to the other regimes and occurs due to lattice vacancies that exist on the surface of the iron. As the surface becomes oxidized, the reaction becomes kinetically limited and the production rate reaches steady state which corresponds to hour 1 in figure 2. As the oxide layer becomes more developed diffusion through the layer to the surface of the iron becomes the limiting affect and the production rate begins to drop which is represented as hour 2 and hour 3. The ideal conditions for the oxidation process exist as a purely kinetic-limited reaction that is attributed to water adsorption. Figure 3 represents the production rate data during 1 hour of oxidation in an effective arrhenius form.

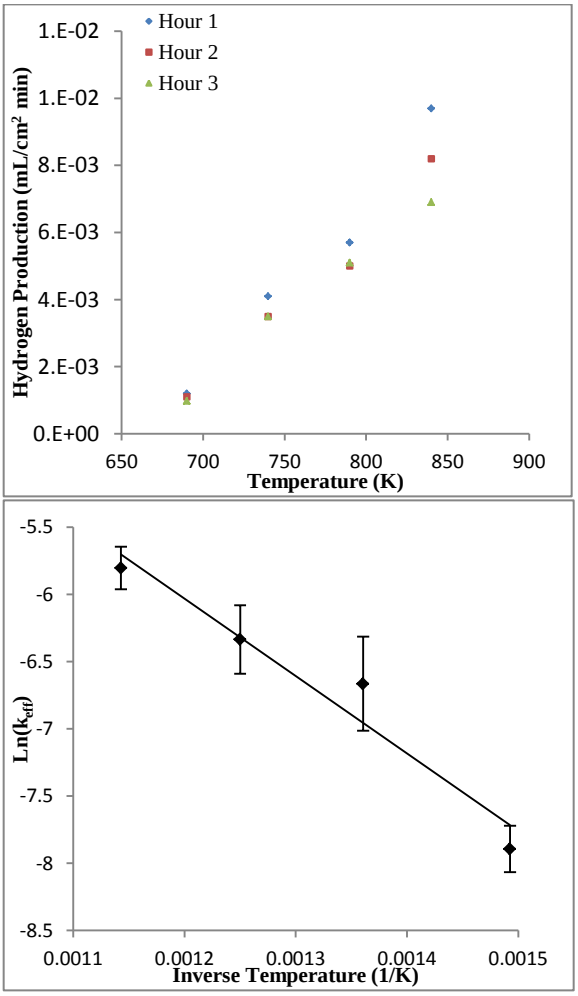

Figure 2: Production Rate vs. Temperature

Figure 7: Arrhenius

The activation energy of 50kJ/mol obtained as a result of the linear fit of the Arrhenius equation shows a strong correlation to the dissociation energy of water via chemisorption onto magnetite. This result suggests that the water dissociation step for the oxidation mechanism is the rate limiting step in the kinetic-limited regime. The next step into the investigation of fundamental reaction kinetics focuses on the reduction step and more importantly the coupling of reduction and oxidation reactions into regenerative cycles. Iron oxide samples were formed by oxidizing iron under the

conditions stated previously for approximately 45 minutes at 790K. Reduction of the iron oxide was done under the same reactor conditions without the flow of water and by replacing nitrogen with carbon monoxide (100cc/min). Cycling between reduction and oxidation was achieved by first exchanging the supply of nitrogen (MWN2=28) under oxidation with helium to prevent confusion during data acquisition with carbon monoxide (MWCO=28) under reduction conditions. The length of an oxidation step was estimated to correspond to production rates that precede the kinetically-limited regime so as to maximize cycling efficiency. Figure 4 shows multiple oxidation steps that lasted 20 minutes following 1 minute of reduction. The 45 minute oxidation period that preceded the cycling process also is represented in the figure to signify where oxidation should be stopped and reduction commence.

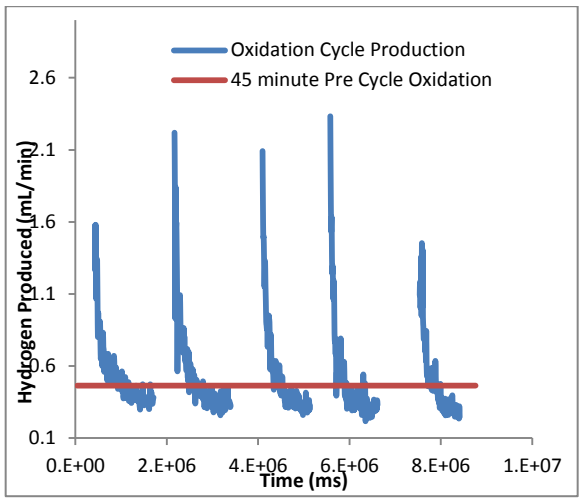

Figure 4: Preliminary Cycling Results

Initial optimization for the cycling process has been estimated for 7 ½ minute cycles for a 75 cycle experiment. Oxidation lasts for about 4 minutes and reduction for 1 minute. Figures 5 and 6 express promising results as future experiments are conducted and further optimization of the cycling process is obtained. Both figures show the amounts of hydrogen produced and carbon dioxide produced for each cycle. Every mole of hydrogen that is formed as a result of oxidation can correlate to a mole of carbon dioxide obtained as a result of reduction. The optimal cycling condition would allow for all lattice vacancies filled during oxidation to be regenerated during reduction. The results in Figures 5 and 6 show carbon dioxide formation at a slightly elevated rate in relation to the amount of hydrogen produced. This may be due to resolution issues within the mass analyzer.

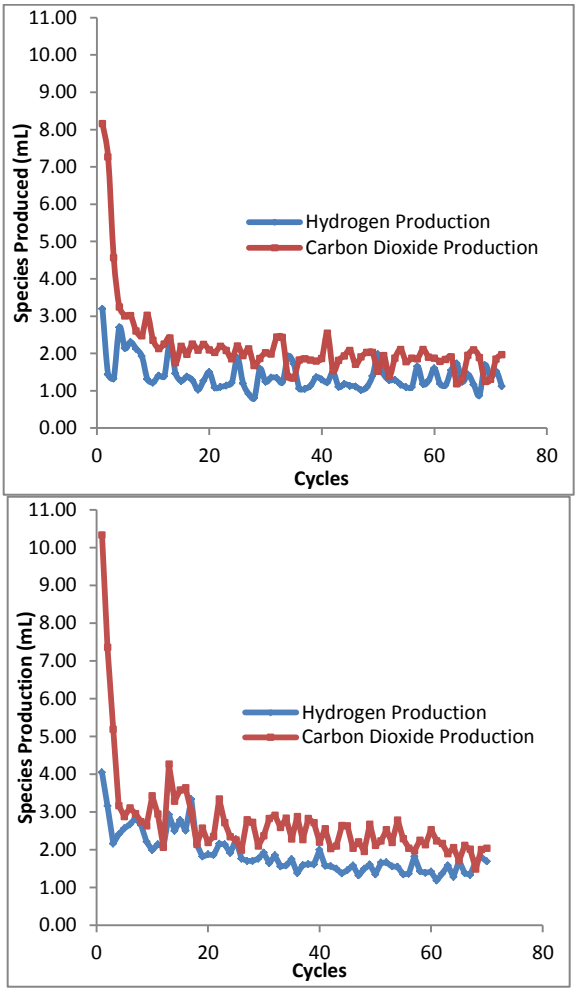

Figures 5 and 6: Species Production For The Oxidation and Reduction Steps.

Another consideration taken into account for cycle optimization is for the reduction and oxidation steps to occur as surface reactions on the oxide layer. This would mean that as water molecules are adsorbed, they do not diffuse through the oxide layer or dissociate under the surface of the oxide. Figure 7 and 8 represent oxygen to iron ratios at different points within the oxide layer. As the oxide layer grows, the ratio of oxygen on the surface should be slightly higher than that at the iron/iron-oxide interface. Figure 7 represents the oxygen ratios after an oxidation and Figure 8 is for post reduction. As you can see under both cases the ratios at the material interface and mid-point of the oxide layer are similar. At the surface however, the reduction shows a lower oxygen ratio. This signifies surface reactions and limited diffusion.

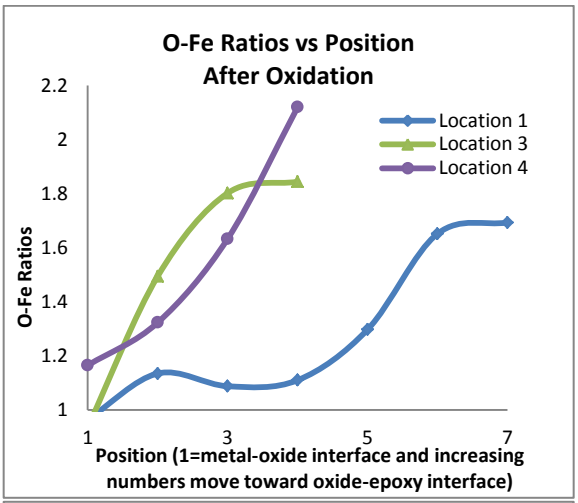

Figure 7: Oxide Ratios after Oxidation.

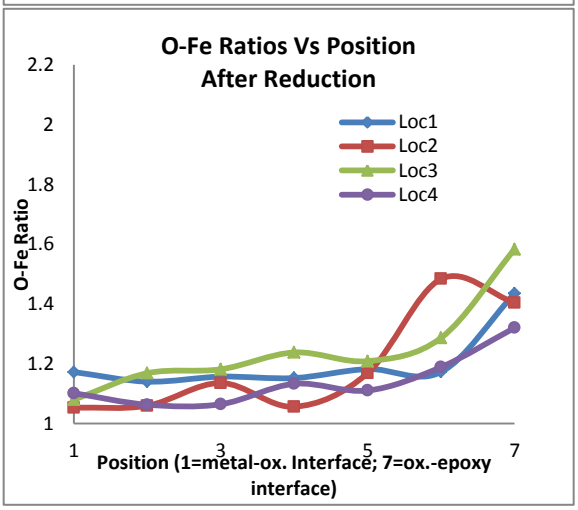

Figure 8: Oxide Ratios sfter Reduction.

As further investigation into the reaction kinetics for the cycling process continues further optimization of the process will be done and repeatable experimental tests will be conducted in order to obtain the fundamental kinetic parameters of the reaction mechanisms. This would include testing different cycling conditions and reconfiguring our mass analyzer. Future work may include identifying and testing alternative reduction techniques.

Fundamental Catalysis Work

X-ray diffraction data was obtained from the two catalysts; 20wt% Fe on n-ZrO_2 and 20wt% Fe on n-$ZrO_2(Y_2O_3)$, after heat treatment at 1500°C for two hours. The XRD patterns obtained from the FeO_x/n-ZrO_2 is presented in Figure 9.

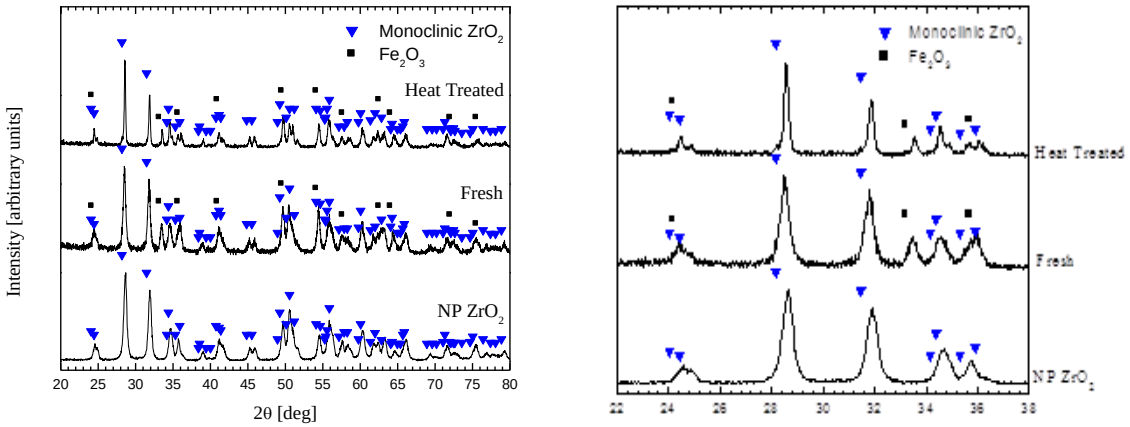

Figure 9: XRD Spectra For 20wt% Iron Deposited On Nanoparticle Zirconium Oxide; (A) Full Range From 2Θ= 20° To 80° And (B) Narrow 2 Θ Range Between 22° And 38° To Reveal Fe2O3 Peaks.

The monoclinic crystal phase of n-ZrO2 is present in all XRD patterns and an increase in ZrO2 particle size is evident in the sharper peaks from the heat treated catalyst. However, the increase in particle size is not as significant as would be expected after a heat treatment at 1500°C. Both the fresh and heat-treated catalysts reveal iron (III) on the surface (Fe2O3). While this suggests that the major iron oxide on both catalysts is Fe2O3, it does not rule out the presence of other oxides or iron metal as they may be below the detection limit of XRD. Particles on the order of 1-2 nm and below are difficult to detect with XRD. The particle sizes for the Fe2O3 on the catalysts were calculated using the peak widths and the Scherrer equation. According to these calculations, the iron oxide particle size increased from 46 nm to 74 nm during the heat treatment. Since a much larger increase in particle size is expected after a heat treatment at 1500°C, this indicates that the n-ZrO2 limits iron oxide particle growth. The XRD patterns obtained from the 20wt% Fe on n-ZrO2 (Y2O3) catalysts before and after heat treatment are presented in Figure 10. The XRD patterns obtained from these catalysts are very different from those obtained from the FeOx/n-ZrO2 catalysts, mainly due to the fact that the ZrO2 is monoclinic in the n-ZrO2-supported catalysts and cubic in the n-ZrO2 (Y2O3)-supported catalysts. The cubic phase has fewer XRD peaks than the monoclinic phase. However, there are other differences between the n-ZrO2- and the n-ZrO2 (Y2O3)-supported catalysts. Compared to the n-ZrO2-supported catalyst, it appears that the ZrO2 particles are significantly larger after heat treatment on the n-ZrO2 (Y2O3)-supported catalyst. Also, the original Fe2O3 peaks are difficult to detect on the heat treated FeOx/n-ZrO2 (Y2O3) catalyst. Instead there is an indication of Fe3O4, i.e. reduction of Fe2O3. It has been noted in literature that iron oxide is incorporated in the lattice of yttria-stabilized zirconia when heated to very high temperatures. This can explain why it is difficult to detect the iron oxide in the XRD patterns obtained from the heat treated FeOx/n-ZrO2 (Y2O3) catalyst. Incorporation of FeOx into the lattice frame work of Y2O3-doped ZrO2 is interesting, if it can minimize sintering of the iron oxide particles.

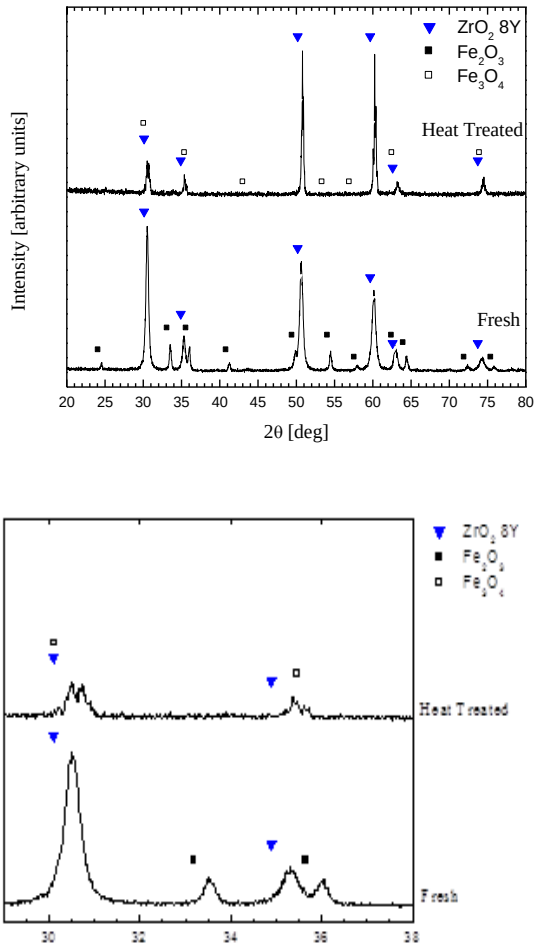

Figure 10: XRD Spectra Obtained From 20wt% Iron Deposited On Yttria-Stabilized Zirconium Oxide; (A) Full Range From 2Θ= 20° To 80° And (B) Narrow 2Θ Range Between 28° And 38°.

The design of a reactor system for testing of the catalysts in the two-step water splitting reaction has been completed (Figure 3). The reactor system requires a high temperature furnace to allow reactions at 1500C. This furnace has been ordered and received. We are in the process of building the rest of the system and are looking into purchasing a mass spectrometer (MS) for continuous monitoring of reaction products.

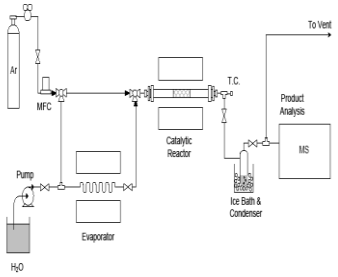

Figure 11: Reactor System Diagram for Both The Oxygen Removal Step And Hydrolysis Step For Two-Step Water-Splitting.